PHYSICAL REVIEW B **79**, 020205(R) (2009)

Nanoscale metastable state exhibiting pseudotenfold diffraction pattern in Fe-based bulk metallic glass

Akihiko Hirata,[1,*] Yoshihiko Hirotsu,[1,2] Kenji Amiya,[3] and Akihisa Inoue[3]

[1]*Institute of Scientific and Industrial Research, Osaka University, Ibaraki, Osaka 567-0047, Japan*

[2]*R&D Institute of Metals and Composites for Future Industries (RIMCOF), Osaka University Laboratory, Ibaraki, Osaka 567-0047, Japan*

[3]*Institute for Materials Research, Tohoku University, Sendai 980-8577, Japan*

(Received 16 November 2008; revised manuscript received 6 January 2009; published 30 January 2009)

We have found nanoscale metastable state with a χ-FeCrMo-like structure exhibiting pseudotenfold diffraction pattern in the course of crystallization in an Fe-based $Fe_{48}Cr_{15}Mo_{14}C_{15}B_6Tm_2$ bulk metallic glass with a high glass stability. All the diffraction spots were found along the first and second halo rings of the glass structure. It was also found that the diffraction pattern with the pseudotenfold symmetry changed into the [113] zone-axis pattern of the χ-FeCrMo structure. On the basis of the results, we discussed local atomic arrangements of this metastable state in relation to the glass stability.

DOI: 10.1103/PhysRevB.79.020205 PACS number(s): 64.70.pe, 61.05.jm, 64.70.dg

Local atomic arrangements of metallic glasses have been intensively addressed by using experimental and computational structural analyses.[1–4] In addition to this, it is widely accepted that atomic arrangements of crystalline or quasicrystalline structures formed in crystallization stage are also important in understanding the local atomic arrangements of metallic glasses. For example, in Zr-based metallic glasses, icosahedral atomic clusters have been suggested to exist as a dominant local atomic arrangement in the glass states[5–8] since icosahedral atomic cluster is known as a basic structural unit of quasicrystal phase and the big-cube phase (Ti_2Ni type) which are formed during the first crystallization process.[9–11] In Fe-based and Pd-based metallic glasses known as metal-metalloid systems, on the other hand, prism-type structures with a central metalloid atom are regarded as dominant structural units when the metalloid composition is beyond 20 at %.[12] In these metallic glasses, Fe_3B, Pd_3P, etc., known as their crystalline phases, are also composed of periodic arrangements of the prism-type structural units. In lower metalloid (B, C, or P) composition range (less than 20 at %), aside from the prism-type structures, crystal structures comprising coordination polyhedra with large coordination numbers (CN) have been reported in crystallization of various Fe-based metallic glasses. For example, as a crystalline phase, the α-Mn-type structure with CN12, CN13, and CN16 polyhedra was reported in Fe-(Cr, Mo, W)-C,[13] Fe-Si-C,[14] Fe-Si-P,[15] Fe-Nb-B,[16] and Fe-Si-Nb-B (Ref. 17) metallic glasses, and the σ-phase structure with CN12, CN14, and CN15 polyhedra was reported in Fe-Si-B and Fe-Cr-V-B metallic glasses.[18] Note that the icosahedral atomic cluster is identical to a coordination polyhedron with CN12. A coordination polyhedron with CN16 can be seen in the $Cr_{23}C_6$-type structure (stoichiometric metalloid composition is 20.7 at %) which is frequently found in crystallization of the Fe-based metallic glasses such as Fe-Nb-B,[16] Fe-Nb-Zr-B,[19] Fe-Nb-B-Y,[20] and (Fe, Co, Ni)-Si-Nb-B (Ref. 21) with metalloid composition larger than 20 at % although the prism-type units are also included in the structure.[22] From these facts, the coordination polyhedra are considered to be also important structural units in Fe-based metallic glasses as well as the prism-type structure. It is a significant issue to solve which kind of local structures and their linkage manners fundamentally contribute to the high glass stability of the Fe-based bulk metallic glasses (BMGs).

Recently, in Fe-based glasses, nonferromagnetic BMGs with a rod diameter of more than 1 cm have been synthesized using a Cu-mold casting method.[23–25] It was found that the glass-forming ability could be drastically improved by adding a small amount of lanthanides to Fe-transition metal-metalloid alloys such as Fe-(Cr, Mo)-(C, B) (Ref. 26). In order to understand the high glass stability, it is significant to reveal the local atomic arrangements and their relation to the growth process of crystalline phases in crystallization. Very recently, we have examined a crystallization process of an $Fe_{48}Cr_{15}Mo_{14}C_{15}B_6Tm_2$ BMG which belongs to the above type of Fe-based BMG with quite high glass stability (the crystallization temperature is as high as 910 K).[22] During the crystallization, double exothermic reactions were found using differential scanning calorimetry (DSC).[25] Although such double peaks were also observed in the same type of Fe-based BMGs,[23,24] only the $Cr_{23}C_6$-type phase was reported as the main crystalline product in the crystallization.[23] In the $Fe_{48}Cr_{15}Mo_{14}C_{15}B_6Tm_2$ glass, we found α-Mn-type χ-FeCrMo structure corresponding to the first peak of the double exothermic DSC peaks.[22] Moreover, before the formation of χ-FeCrMo, χ-FeCrMo-like long period structures (LPSs) were also observed in nanoscale as small as 5 nm.[22] From such nanoscale regions, we have successfully obtained pseudotenfold electron-diffraction patterns such as quasicrystal using nanobeam electron diffraction (NBED). In this Rapid Communication, we present the obtained experimental results and discuss the atomic arrangement by comparing with the χ-FeCrMo structure.

A ribbon of the $Fe_{48}Cr_{15}Mo_{14}C_{15}B_6Tm_2$ metallic glass was made by using the single-roll rapid quenching technique. In order to observe the crystallization process by transmission electron microscopy (TEM), the ribbon specimens were annealed isothermally at 893, 923, and 973 K for 30 min in a vacuum furnace. Specimens for TEM observation were prepared by electropolishing (acetic-perchloric acid) at room temperature. The surface oxide layer was removed using the Ar ion-milling technique at a voltage of 3 keV under a low

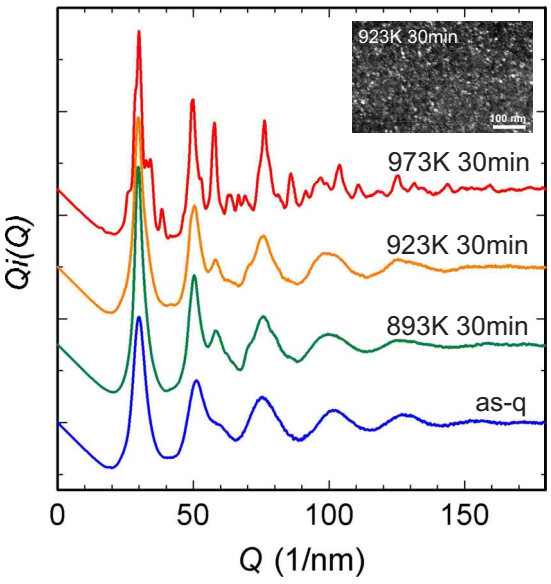

FIG. 1. (Color online) Reduced interference functions $Qi(Q)$ obtained from electron-diffraction patterns of as-quenched and annealed specimens. A dark field image obtained from the specimen annealed at 923 K is also shown in the inset.

glancing angle of 4° (GATAN PIPS). Selected area electron-diffraction (SAED) patterns for obtaining reduced interference functions $Qi(Q)$ were taken using a LEO-922D TEM (200 kV) equipped with an omega-type energy filter. The SAED patterns were recorded on imaging plates (IP) and read by using an IP reader (DITABIS MICRON). NBED patterns were taken using a JEM-3000F TEM (300 kV). NBED patterns were captured using a television rate video camera by scanning a nanoprobe (diameter: ~1 nm) at a speed of ~10 nm/s. More than 50 000 frames were recorded on the video tape and relatively clear patterns were selected for analyzing local structures of the nanoscale regions. The amount of electron dose for the nanoprobe in NBED was 2.0×10^{19} e/cm^2 (measured by a Faraday gauge), almost ten times smaller than that for the conventional high-resolution electron microscopy imaging.

Figure 1 shows four $Qi(Q)$ profiles obtained from the as-quenched specimen and the specimens annealed at 893, 923, and 973 K for 30 min. Here, $i(Q)$ denotes the interference function, and Q is the scattering vector defined as $Q=4\pi\sin\theta/\lambda$, where θ is the scattering angle and λ is the electron wavelength. A procedure for obtaining the $i(Q)$ curve from the SAED patterns was described in our previous paper.[27] With increasing the annealing temperature, the $Qi(Q)$ profile gradually changed along with an appearance of many subpeaks. At 973 K, apparent crystalline peaks can be seen in the profile and it was reveled that all the peaks come from the $Cr_{23}C_6$-type structure as was described in the previous paper.[22] The χ-FeCrMo-like LPSs were observed in the specimens annealed at 893 and 923 K where $Qi(Q)$ profiles similar to that from the as-quenched specimen were obtained. The χ-FeCrMo structure (α-Mn type) was found only in the specimen annealed at 923 K. In addition, a dark field image obtained from the specimen annealed at 923 K (using a part of the first Debye ring) is also shown in the inset.

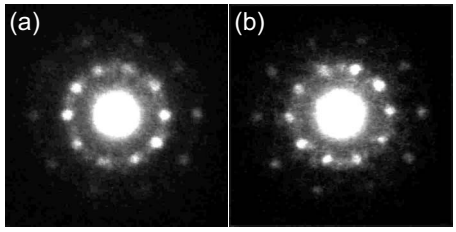

FIG. 2. Pseudotenfold NBED patterns obtained from the specimen annealed at 923 K for 30 min. The patterns (a) and (b) were taken from different areas. The pattern of (a) is close to exact tenfold symmetry whereas the pattern of (b) is slightly distorted.

From the image, grain sizes are less than 10 nm at this stage.

Characteristic two types of NBED patterns with pseudotenfold symmetry obtained from the specimen annealed at 923 K are shown in Figs. 2(a) and 2(b). The NBED patterns (a) and (b) were taken from different nanoscale regions. Interestingly, we can see pseudotenfold diffraction patterns with ten strong diffraction spots along the first and second halo rings in both the patterns. Note that pattern (a) is close to exact decagonal symmetry, whereas pattern (b) is slightly distorted from exact one. Therefore, it is considered that the structure giving pattern (a) is more close to the glass structure. Even in pattern (a), however, distances between neighboring diffraction spots observed on the first halo ring were found to be fluctuated within 10%. In this Rapid Communication, the local structural state especially exhibiting pseudotenfold NBED pattern is called the χ' state.

In the specimen annealed at 923 K, we also found deformed tenfold NBED patterns as shown in Fig. 3(a). This pattern was found to be similar to the [113] zone-axis pattern of the χ-FeCrMo structure as simulated in Fig. 3(c). For comparison, an experimental NBED pattern obtained from the χ-FeCrMo structure is also shown in Fig. 3(b). In Fig. 3(a), it can be seen that positions of the diffraction spots indicated by A and B deviate from the positions forming the tenfold arrangement. This feature of diffraction spot positions is quite similar to that in the [113] pattern of χ-FeCrMo for those spots beside the $33\bar{2}$ or $\bar{3}\bar{3}2$ spot, as indicated by arrow heads in Fig. 3(b). The NBED pattern in Fig. 3(a) is intermediate characteristics between the pseudotenfold pattern of the χ' state (Fig. 2) and the [113] pattern of the χ-FeCrMo structure [Fig. 3(b)]. From this fact, the χ' state with the pseudotenfold pattern can be regarded as a precursor state before forming χ-FeCrMo.

In order to understand the χ' state in detail, we here focus on an atomic arrangement of the χ-FeCrMo structure. Figure 4 shows the [113] projection of the χ-FeCrMo structure with respect to a Mo framework. All the atoms projected on (113) including Fe and Cr atoms are depicted in the upper left portion. A linkage of pentagonal tiles is arranged in a periodic manner. Note that Mo atoms are always central atoms of all the CN16 polyhedra and the [113] projection of Mo exhibits a pentagonal tile pattern. This structure can be explained by only three linkage manners of the pentagonal tiles with three limited angles as shown in Fig. 4(b). Anisotropic feature of the [113] pattern that largely deviates from the decagonal symmetry presumably comes from the limited

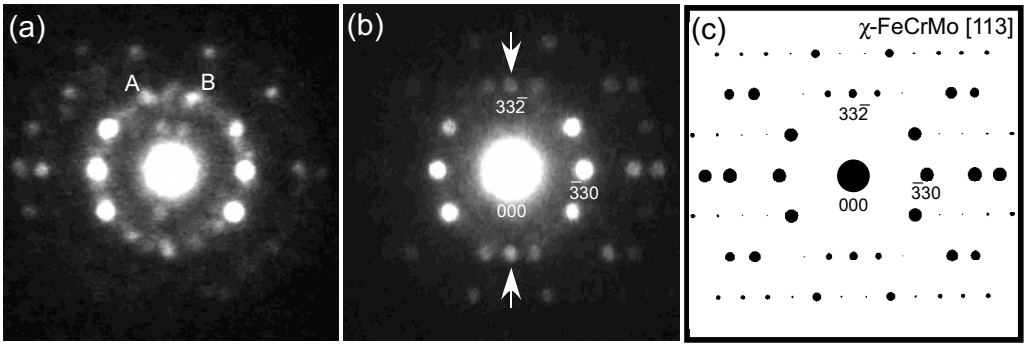

FIG. 3. (a) Deformed tenfold NBED pattern obtained from the specimen annealed at 923 K for 30 min, together with an [113] zone-axis (b) experimental and (c) calculated patterns.

linkage manners (only three directions). To achieve the tenfold symmetry, additional two tiles are considered to be necessary [Fig. 4(c)]. Considering this fact, we tried to construct a projection of a preliminary structural model projected along the direction corresponding to [113] of the χ structure as shown in Fig. 4(d). The model consists entirely of the five directional linkages of the pentagonal tiles which are shown in both Figs. 4(b) and 4(c). The atomic arrangement in each tile is just identical to that in the χ-FeCrMo structure. However, it is necessary to modify the atomic positions and replace some Fe, Cr, and Mo atoms with C, B, and Tm atoms.

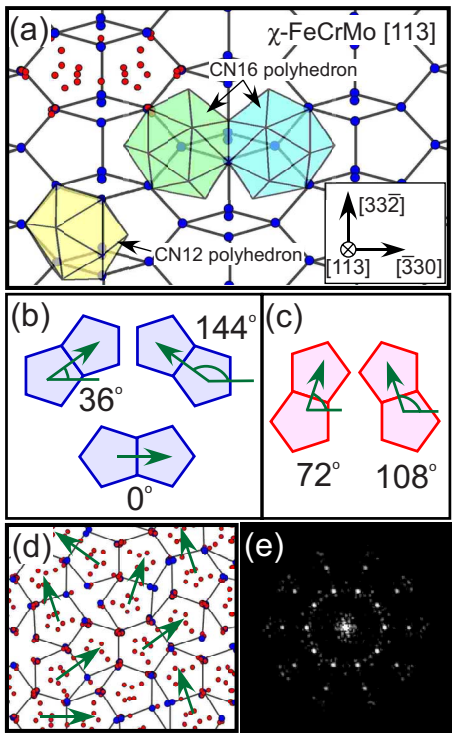

FIG. 4. (Color online) (a) [113] projection of the χ-FeCrMo structure with respect to the Mo linkage in which the pentagonal tiles are arranged regularly. All the atoms including Fe and Cr are shown at the upper left. (b) Three tiling manners of pentagonal tiles found in the χ-FeCrMo structure, and (c) another tiling manner which are necessary to make the tenfold symmetry. (d) Preliminary structure model of the χ' state including five tiling manners and (e) fast Fourier transform pattern obtained from the model.

A fast Fourier transform pattern obtained from the model is also shown in Fig. 4(e). The pattern is well consistent with the experimental one (Fig. 2). Although the present structural model is just a projected structure model, the basic concept of adding the additional two tiles is considered to be adequate. To reveal the atomic arrangement, it is inevitable to elucidate more structural details from analyses in both the reciprocal and real spaces. Unfortunately, however, it is difficult to obtain correct structural information at present since the regions are quite small (~5 nm) and are oriented randomly.

The linkage of Mo atoms is directly related to that of CN16 polyhedra since CN16 polyhedra are always formed surrounding the Mo atoms in the χ-FeCrMo structure. It is likely that the structural difference between the χ' and χ-FeCrMo structures is characterized by the linkage manner of CN16 polyhedra. Because of the additional two tiles to the χ-FeCrMo structure, it is expected that the χ' state has more variety of the linkage manners concerning the polyhedra compared with χ-FeCrMo. Since the glass structure is similar to the χ' structure (in both of the states, the strong NBED spots can be seen just on the halo rings[22]), it is expected that various stable linkages of the polyhedra are also found in the glass state as a medium range order (MRO) structure. Due to great flexibility of the linkages, possible stable MRO structures that conform to the halo diffraction intensity are probably increased in the present BMG compared with less-stable metallic glasses. The locally stabilized MRO structures are considered to resist the atomic rearrangement toward the crystallization. We infer from these speculations that the quasicrystal-like local structure plays an important role for stabilizing the glass state.

Previously, among Fe-based alloys, the diffraction pattern with tenfold symmetry has been reported only in crystalline alloys.[28–31] One of us (A.H.) and Koyama found a disordered decagonal atomic column state in solid solution of an Fe-Mo alloy where deformed decagonal atomic columns are linked to each other in ten different directions.[31] This state is partly similar to quasicrystal in that there is bond-orientational order but quasiperiodic order is low. The χ' state found in this study (see Fig. 2) probably belongs to the same sort of structure because there is no strong ordered spot with lower scattering angle (inside of the first halo ring), which is usually observed in the diffraction patterns from quasicrystal. No such bond-orientational-ordered structure partly similar to

quasicrystal has been reported for Fe-based metallic glasses. However, in this study, we found the quasicrystal-like χ' state in the $Fe_{48}Cr_{15}Mo_{14}C_{15}B_6Tm_2$ BMG with an extremely high glass stability. A close relationship between quasicrystal and BMG formations has been discussed by Dong *et al.*,[32] based on phase diagrams. They pointed out that both quasicrystal and BMG alloy systems have a similar compositional rule for their formations in the phase diagrams. The rule is closely related to an existence of the special dense-packed atomic clusters. Also in the present Fe-based alloy, it was confirmed that a good BMG-forming composition well corresponds to a quasicrystal-forming composition.

The appearance of the χ' state with pseudotenfold symmetry reminds us of the quasicrystal formation in Zr-based BMGs. In the Zr-Ti-Ni-Cu-Be BMGs with various alloy compositions, Waniuk *et al.*[33] showed that the icosahedral quasicrystal phases formed for all investigated alloys during the first reaction of the double exothermic reaction at low temperatures. This situation is quite similar to the case of the present alloy as was mentioned. In both cases, moreover, calorific values of the first exothermic reaction are smaller than those of the latter one.[33,34] This fact implies that the quasicrystal(-like) structures are closer to the glass structures in their atomic arrangements compared with those in the crystalline phase(s) which corresponds to the second large DSC peak.

We found metastable χ' state with pseudotenfold symmetry in the course of crystallization in the $Fe_{48}Cr_{15}Mo_{14}C_{15}B_6Tm_2$ BMG. The χ' state was found to change into χ-FeCrMo through a formation of the intermediate χ-FeCrMo-like state. On the basis of the χ-FeCrMo structure, we proposed a preliminary structure model of the χ' state where pentagonal tiles such as χ-FeCrMo are connected to each other in five different directions. It is considered that the χ' state is somewhat similar to quasicrystal in that it has bond-orientational order. This structural state can be regarded as an intermediate one between glass and crystalline states. Therefore, the quasicrystal-like χ' state, which comprises coordination polyhedra, will be helpful for understanding the MRO structure in the BMG.

A.H. acknowledges support from the Ministry of Education, Culture, Sports, Science, and Technology of Japan (Grant No. 20760442). A.H. would also like to sincerely thank A. Koreeda for his technical assistance.

*Corresponding author; ahirata@sankan.osaka-u.ac.jp

[1] E. Matsubara and Y. Waseda, Mater. Trans., JIM **36**, 883 (1995).
[2] Y. Hirotsu, T. Ohkubo, and M. Matsushita, Microsc. Res. Tech. **40**, 284 (1998).
[3] Y. Waseda, H. S. Chen, K. T. Jacob, and H. Shibata, Sci. Technol. Adv. Mater. **9**, 023003 (2008).
[4] H. W. Sheng, W. K. Luo, F. M. Alamgir, J. M. Bai, and E. Ma, Nature (London) **439**, 419 (2006).
[5] T. Takagi, T. Ohkubo, Y. Hirotsu, B. S. Murty, K. Hono, and D. Shindo, Appl. Phys. Lett. **79**, 485 (2001).
[6] J. Saida and A. Inoue, J. Non-Cryst. Solids **317**, 97 (2003).
[7] T. Fukunaga, K. Itoh, T. Otomo, K. Mori, M. Sugiyama, H. Kato, M. Hasegawa, A. Hirata, Y. Hirotsu, and A. C. Hannon, Mater. Trans. **48**, 1698 (2007).
[8] X. Hui, H. Z. Fang, G. L. Chen, S. L. Shang, Y. Wang, and Z. K. Liu, Appl. Phys. Lett. **92**, 201913 (2008).
[9] U. Köster, J. Meinhardt, S. Roos, and H. Liebertz, Appl. Phys. Lett. **69**, 179 (1996).
[10] C. Li and A. Inoue, Phys. Rev. B **63**, 172201 (2001).
[11] K. Kajiwara, M. Ohnuma, T. Ohkubo, D. H. Ping, and K. Hono, Mater. Sci. Eng., A **738**, 375 (2004).
[12] M. Imafuku, S. Sato, E. Matsubara, and A. Inoue, J. Non-Cryst. Solids **312-314**, 589 (2002).
[13] A. Inoue, T. Iwadachi, T. Minemura, and T. Masumoto, Trans. Jpn. Inst. Met. **22**, 197 (1981).
[14] Y. C. Chen, C. M. Chen, K. C. Su and K. Yang, Mater. Sci. Eng., A **133**, 596 (1991).
[15] M. Ohnuma, O. Sasaki, H. Kuwano, S. Katano, Y. Morii, S. Funahashi, H. R. Child, and Y. Hamaguchi, Mater. Trans., JIM **34**, 874 (1993).
[16] M. Imafuku, S. Sato, H. Koshiba, E. Matsubara, and A. Inoue, Scr. Mater. **44**, 2369 (2001).
[17] I. V. Lyasotskii, N. B. Dyakonova, E. N. Vlasova, D. L. Dyakonov, and M. Yu. Yazvitskii, Physiol. Rev. **203**, 259 (2005)
[18] N. B. Dyakonova, I. V. Lyasotskii, E. N. Vlasova, D. L. Dyakonov, and B. V. Molotilov, Adv. Perform. Mater. **4**, 199 (1997).
[19] M. Shapaan, J. Lábár, J. Lendvai, L. K. Varga, Mater. Sci. Eng., A **357-377**, 789 (2004).
[20] D. H. Kim, J. M. Park, D. H. Kim, and W. T. Kim, J. Mater. Res. **22**, 471 (2007).
[21] A. Inoue, B. L. Shen, and C. T. Chang, Intermetallics **14**, 936 (2006).
[22] A. Hirata, Y. Hirotsu, K. Amiya, and A. Inoue, Phys. Rev. B **78**, 144205 (2008).
[23] V. Ponnambalam, S. J. Poon, and G. J. Shiflet, J. Mater. Res. **19**, 1320 (2004).
[24] Z. P. Lu, C. T. Liu, J. R. Thompson, and W. D. Porter, Phys. Rev. Lett. **92**, 245503 (2004).
[25] K. Amiya and A. Inoue, Mater. Trans. **47**, 1615 (2006).
[26] S. Pang, T. Zhang, K. Asami, and A. Inoue, Mater. Trans. **42**, 376 (2001).
[27] A. Hirata, Y. Hirotsu, T. Ohkubo, T. Hanada, and V. Z. Bengus, Phys. Rev. B **74**, 214206 (2006).
[28] Z. W. Hu, X. L. Jiang, J. Zhu, and S. S. Hsu, Philos. Mag. Lett. **61**, 115 (1990).
[29] P. Liu, A. H. Stigenberg, and J.-O. Nilsson, Acta Metall. Mater. **43**, 2881 (1995).
[30] K. Yamamoto, Y. Kimura, and Y. Mishima, Mater. Trans. **45**, 357 (2004).
[31] A. Hirata and Y. Koyama, Phys. Rev. B **70**, 134203 (2004).
[32] C. Dong, Q. Wang, J. B. Qiang, Y. M. Wang, N. Jiang, G. Han, Y. H. Li, J. Wu, and J. H. Xia, J. Phys. D **40**, R273 (2007).
[33] T. Waniuk, J. Schroers, and W. L. Johnson, Phys. Rev. B **67**, 184203 (2003).
[34] I. Martin, T. Ohkubo, M. Ohnuma, B. Deconihout, and K. Hono, Acta Mater. **52**, 4427 (2004).